




A Chimeric *Plasmodium vivax* Merozoite Surface Protein Antibody Recognizes and Blocks Erythrocytic *P. cynomolgi* Berok Merozoites *In Vitro*

Fei-hu Shen,^a Jessica Jie Ying Ong,^b Yi-fan Sun,^a Yao Lei,^a Rui-lin Chu,^a Kokouvi Kassegne,^a Hai-tian Fu,^a Cheng Jin,^c Eun-Taek Han,^d Bruce Russell,^b Jin-Hee Han,^{b,d}  Yang Cheng^a

^aLaboratory of Pathogen Infection and Immunity, Department of Public Health and Preventive Medicine, Wuxi School of Medicine, Jiangnan University, Wuxi, Jiangsu, People's Republic of China

^bDepartment of Microbiology and Immunology, University of Otago, Dunedin, New Zealand

^cDepartment of Hepatobiliary Surgery, Affiliated Hospital of Jiangnan University (Wuxi Third People's Hospital), Wuxi, Jiangsu, People's Republic of China

^dDepartment of Medical Environmental Biology and Tropical Medicine, School of Medicine, Kangwon National University, Chuncheon, Gangwon-do, Republic of Korea

Fei-hu Shen, Jessica Jie Ying Ong, and Yang Cheng contributed equally to this work. Author order was determined on the basis of seniority.

ABSTRACT Research on erythrocytic *Plasmodium vivax* merozoite antigens is critical for identifying potential vaccine candidates in reducing *P. vivax* disease. However, many *P. vivax* studies are constrained by its inability to undergo long-term culture *in vitro*. Conserved across all *Plasmodium* spp., merozoite surface proteins are essential for invasion into erythrocytes and highly expressed on erythrocytic merozoites, thus making it an ideal vaccine candidate. In clinical trials, the *P. vivax* merozoite surface protein 1 (PvMSP1-19) vaccine candidate alone has shown to have limited immunogenicity in patients; hence, we incorporate the highly conserved and immunogenic C terminus of both *P. vivax* merozoite surface protein 8 (PvMSP8) and PvMSP1-19 to develop a multicomponent chimeric protein rPvMSP8+1 for immunization of mice. The resulted chimeric rPvMSP8+1 antibody was shown to recognize native protein MSP8 and MSP1-19 of mature *P. vivax* schizonts. In the immunized mice, an elevated antibody response was observed in the rPvMSP8+1-immunized group compared to that immunized with single-antigen components. In addition, we examined the growth inhibition of these antibodies against *Plasmodium cynomolgi* (Berok strain) parasites, which is phylogenetically close to *P. vivax* and sustains long-term culture *in vitro*. Similarly, the chimeric anti-rPvMSP8+1 antibodies recognize *P. cynomolgi* MSP8 and MSP1-19 on mature schizonts and showed strong inhibition *in vitro* via growth inhibition assay. This study provides support for a new multiantigen-based paradigm rPvMSP8+1 to explore potential chimeric vaccine candidates against *P. vivax* malaria using sister species *P. cynomolgi*.

KEYWORDS *Plasmodium vivax*, merozoite surface proteins, *Plasmodium cynomolgi*, growth inhibition assay, immunogenicity, vaccine candidate

Malaria remains the most common and devastating mosquito-borne disease in the world. It poses a significant threat to public health and has restricted the development of social economy. *Plasmodium falciparum* and *Plasmodium vivax* are the major causes of malaria in humans. In 2018, the proportion of malaria cases caused by *P. falciparum* was 99.7% in Africa, whereas that caused by *P. vivax* was 75% and 53% in South American and Southeast Asian regions, respectively (1). In China, the launch of the China Malaria Elimination Action Plan (2010 to 2020) led to a decline in malaria cases with no indigenous cases reported in 2017 (2, 3). However, imported cases of malaria have been reported in China and, if untreated, can be a potential threat to

Citation Shen F-H, Ong JJY, Sun Y-F, Lei Y, Chu R-L, Kassegne K, Fu H-T, Jin C, Han E-T, Russell B, Han J-H, Cheng Y. 2021. A chimeric *Plasmodium vivax* merozoite surface protein antibody recognizes and blocks erythrocytic *P. cynomolgi* Berok merozoites *in vitro*. *Infect Immun* 89:e00645-20. <https://doi.org/10.1128/IAI.00645-20>.

Editor Jeroen P. J. Saeij, UC Davis School of Veterinary Medicine

Copyright © 2021 American Society for Microbiology. All Rights Reserved.

Address correspondence to Jin-Hee Han, han.han@kangwon.ac.kr, or Yang Cheng, woerseng@126.com.

Received 13 October 2020

Accepted 14 October 2020

Accepted manuscript posted online 16 November 2020

Published 19 January 2021

human health (4). For *P. vivax*, the use of antimalarial drugs, such as chloroquine, is effective at ridding blood-stage malaria, but the recent emergence of chloroquine-resistant *P. vivax* parasites complicates the control of malaria infections (5). Thus, the investigation of alternative approaches to combat *P. vivax*, such as the development of an effective malaria vaccine, is in urgent need. The ideal vaccine design would target all stages of the *Plasmodium* life cycle, which includes preerythrocytic, erythrocytic, and transmission stages. It is widely believed that a vaccine that delivers immunogenicity against multiple stages of parasite development would confer better protection. Currently, two *P. vivax* preerythrocytic vaccines (VMP001 and LSP) showed safety and immunogenicity in malaria-naïve volunteers (6, 7), while vaccines targeting blood-stage infection may form a complementary approach to vaccines against the other life cycle stages that aim to control and clear parasitemia.

In the blood stage, malaria parasites invade host cells through the contact between merozoites and erythrocytes; during this process, the gauzy merozoite coat makes first contact (8). This coat consists of several integral membrane proteins, such as merozoite surface protein 1 (MSP1) (9), MSP2 (10), MSP4 (11), MSP5 (12), MSP8 (13), and MSP10 (14). MSP1, essential for erythrocyte invasion, is the most abundant protein located on the merozoite surface and is a promising blood-stage vaccine candidate. Upon activation, the MSP1 complex is cleaved into four fragments (83, 30, 38, and 42 kDa) (15). The 42-kDa polypeptide is cleaved further into two fragments (33 and 19 kDa), and only the 19-kDa glycosylphosphatidylinositol (GPI)-linked fragment (MSP1-19) is retained during merozoite entry (16). Previous studies have shown PfMSP1-19-specific antibodies to effectively inhibit merozoite invasion in monkeys (17). However, the PvMSP1-19 vaccine candidate alone was shown to have limited immunogenicity in patients (18). Thus, to address this limitation, the present study examined the efficiency of MSP8 as a fusion partner for MSP1-19. MSP8 was initially identified in *Plasmodium yoelii*; it has a signal sequence at the N terminus, a GPI anchor, and two epidermal growth factor (EGF)-like domains at the C terminus with similar homology to MSP1 (19). A previous study demonstrated that recombinant *P. falciparum* MSP8 could bind specifically to membrane surface receptors on human erythrocytes, and anti-PfMSP8 antibodies significantly inhibited *P. falciparum* merozoite invasion to erythrocytes (20). In *P. vivax*, MSP8 induces both humoral and cellular immune responses in malaria patients (21). Therefore, the chimeric MSP8 and MSP1-19 recombinant proteins may be a promising and worthwhile attempt in developing a vaccine.

In *P. yoelii*, immunization with the chimeric rPyMSP-1/8 based on MSP8 and MSP1-19 markedly enhances protection against *P. yoelii* 17XL malaria relative to immunization with a single antigen (22). Moreover, in *P. falciparum*, the PfMSP1/8 based on PfMSP8 and PfMSP1-19 can induce high titers of parasite growth inhibitory antibodies (23). However, reports focusing on *P. vivax* are limited. In the present study, we constructed *P. vivax* merozoite surface protein 8 (PvMSP8) partial peptides, which were highly reactive to *P. vivax* patient serum samples and PvMSP8-specific antibodies, fused to PvMSP1-19 into a novel chimeric protein (rPvMSP8+1). Immune responses against single antigen PvMSP8 (rPvMSP8) or PvMSP1-19 (rPvMSP1-19) and chimeric rPvMSP8+1 in mice were measured. As there is a lack of sustainable long-term *P. vivax* *in vitro* culture, we examined the inhibition of *P. vivax* antibodies using sister species *Plasmodium cynomolgi*, which is the sister taxon of *P. vivax*; shares similar phenotypic, biologic, and genetic characteristics; and is an ideal model system for investigating *P. vivax* biology, evolution, and pathology (24, 25). Hence, we examined the inhibition concentration of rPvMSP8, rPvMSP1-19, and rPvMSP8+1 polyclonal antibodies to *P. cynomolgi* merozoite invasion via *in vitro* growth inhibition assays.

RESULTS

Characterization, expression, and purification of rPvMSP8, rPvMSP1-19, and rPvMSP8+1. PvMSP8 consists of a signal peptide (SP) (amino acids [aa] 1 to 23), an asparagine-rich domain (aa 25 to 123), two EGF-like domains (aa 383 to 463), and a GPI-anchored domain (aa 464 to 486) (Fig. 1A). PvMSP1, which also contains an SP in the N

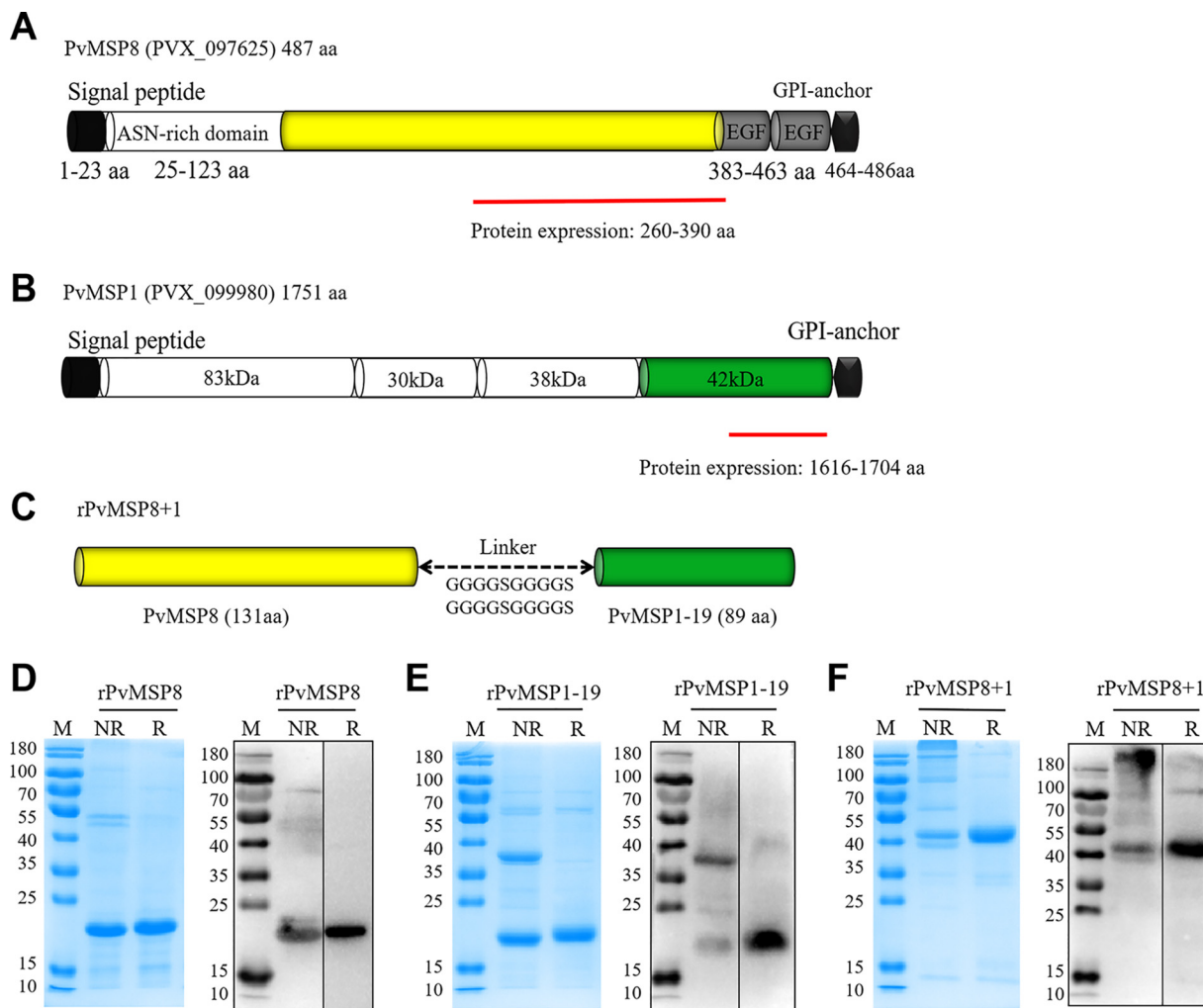


FIG 1 Schematic of PvMSP8, PvMSP1, and rPvMSP8+1 construction. (A) Schematic of PvMSP8. The PvMSP8 protein (encoded by PVX_097625) contains 487 aa with a predicted structure of an SP (aa 1 to 23), a GPI anchor (aa 464 to 486), an asparagine-rich region (ASN; aa 25 to 123), and two EGF-like domains (aa 383 to 463). A truncated PvMSP8 (aa 260 to 399) was constructed for expression. (B) Schematic of PvMSP1. The PvMSP1 protein (encoded by PVX_099980) contains 1,751 aa with a predicted structure of an SP, a GPI anchor, and four fragments of 83, 30, 38, and 42 kDa. A 19-kDa C-terminal fragment (aa 1616 to 1704) was constructed for expression. (C) Schematic of rPvMSP8+1. The rPvMSP8+1 protein consists of 131 aa at the C terminus of MSP8 and 89 aa at the C terminus of MSP1 with a predicted molecular weight of 46 kDa, between which a glycine serine linker (GGGGSGGGGS) was added. (D, E, F) Purified rPvMSP8 (D), rPvMSP1-19 (E), and rPvMSP8+1 (F) were analyzed by SDS-PAGE (12% gel electrophoresis) under both reducing (R) and nonreducing (NR) conditions, followed by Coomassie blue stain and immunoblot analysis using anti-His antibody. M, molecular size marker.

terminus and a GPI-anchored domain in the C terminus, was divided into four different sized segments as follows: PvMSP1-83, PvMSP1-30, PvMSP1-38, and PvMSP1-42. In addition, PvMSP1-42 was divided into two segments as follows: PvMSP1-33 and PvMSP1-19 (Fig. 1B). To synthesize chimeric rPvMSP8+1, a region spanning 131 amino acid residues (aa 260 to 390) of PvMSP8 (rPvMSP8) and 89 amino acid residues (aa 1616 to 1704) of PvMSP1 (rPvMSP1-19) was cloned into the pET32a plasmid with a glycine-serine linker (GGGGSGGGGS) (Fig. 1C).

The single MSP recombinant proteins, rPvMSP8 and rPvMSP1-19, were inserted into the pET30a expression vector, which contains six-histidine residues at the N- and C-terminal ends, respectively. The rPvMSP8, rPvMSP1-19, and rPvMSP8+1 proteins were successfully expressed and purified under nondenaturing conditions. The quality of the purified proteins was assessed by SDS-PAGE stained with Coomassie blue or determined via immunoblot analysis using anti-His antibody. The purified rPvMSP8 migrated as a single band at ~23 kDa under reducing conditions, and no aggregates

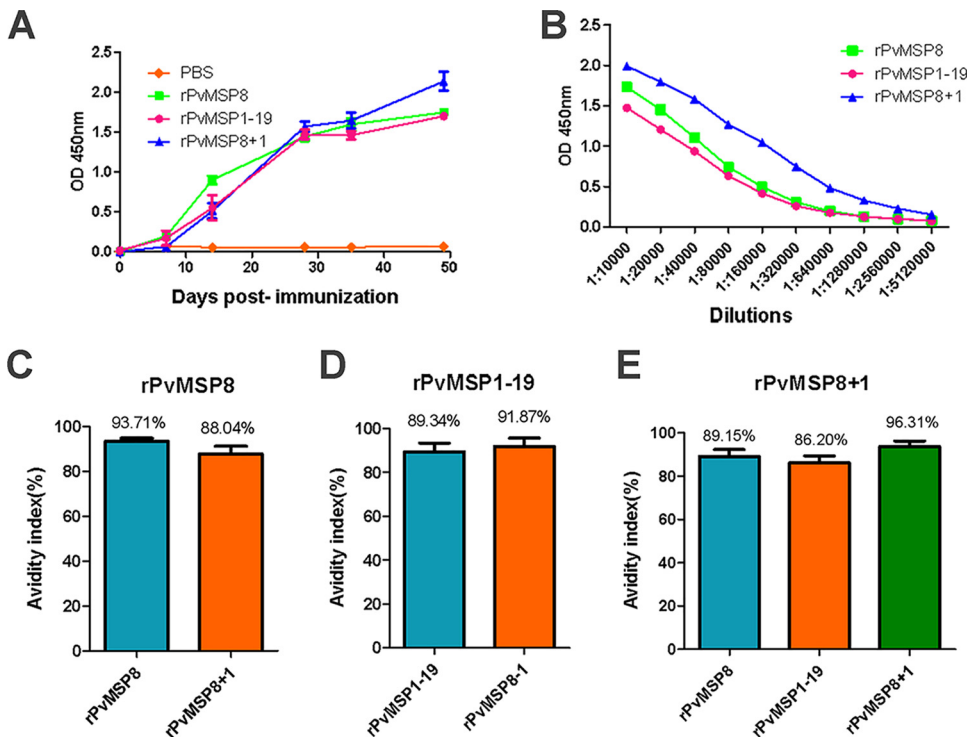


FIG 2 Immune responses in mice immunized with rPvMSP8, rPvMSP1-19, or rPvMSP8+1. (A) IgG levels in rPvMSP8-, rPvMSP1-19-, and rPvMSP8+1-immunized mice. IgG was detected at day 7 postimmunization, and the levels increased throughout the whole immunization period. Antigen specificity was confirmed using preimmune serum samples as controls. (B) Data are presented as the geometric mean OD obtained at different concentrations, expressed as the reciprocal of the serum dilution obtained from mice immunized with rPvMSP8, rPvMSP1-19, or rPvMSP8+1 (dilutions from 1:10,000 to 1:5,120,000). Numbers on the x axis indicate the dilutions tested. (C) Avidity of anti-rPvMSP8 IgG antibodies to rPvMSP8 or rPvMSP8+1 antigen. (D) Avidity of anti-rPvMSP1-19 IgG antibodies to rPvMSP1-19 or rPvMSP8+1 antigen. (E) Avidity of anti-rPvMSP8+1 IgG antibodies to rPvMSP8, rPvMSP1-19, or rPvMSP8+1 antigen.

were observed under nonreducing conditions (Fig. 1D). However, the refolded rPvMSP1-19 migrated as a single protein band at ~18 kDa under reducing conditions and show two bands at ~18 and 36 kDa under nonreducing conditions (Fig. 1E). The larger ~36 kDa rPvMSP1-19 protein band represents a dimer, which could also be recognized by the anti-His antibody. Similarly, the rPvMSP8+1 protein showed a single band at ~42 kDa under reducing conditions but contained a mixture of monomeric and high-molecular-mass bands under nonreducing conditions (Fig. 1F).

Immune response against rPvMSP8, rPvMSP1-19, and rPvMSP8+1 in mice. To generate PvMSP antibodies, four groups of five mice were immunized with rPvMSP8, rPvMSP1-19, rPvMSP8+1, and phosphate-buffered saline (PBS) (negative control), respectively. Using enzyme-linked immunosorbent assay (ELISA), the amount of antibodies generated against the recombinant proteins was examined up to 50 days postimmunization. Mice that received rPvMSP8, rPvMSP1-19, and rPvMSP8+1 generated an immunogenic response 1 week after the primary booster to their received proteins. A high immune response was detected 14 days after immunization and continued to rise throughout the immunization process (Fig. 2A). Mean serum antibody titers were also evaluated 49 days after the first immunization by ELISA. Similarly, rPvMSP8 and rPvMSP1-19 induced a high antibody response with endpoint titers ranging from 1:10,000 to 1:5,120,000. Interestingly, a slightly elevated antibody response with endpoint titers was observed in the rPvMSP8+1-immunized group (Fig. 2B).

In this study, IgG antibodies induced in all mouse groups immunized with adjuvant formulations exhibited high avidity index (AI), which represents the percentage of IgG

antibody bound to the antigen after denaturation treatment with 6 M urea. The highest IgG avidity response was detected in mice immunized with rPvMSP8+1 (mean, 96.31%) compared with those of rPvMSP8 (mean, 93.71%) and rPvMSP1-19 (mean, 89.34%). Anti-rPvMSP8+1 immune serum also had a high IgG avidity response with rPvMSP8 (mean, 88.04%) and rPvMSP1-19 (mean, 91.87%) (Fig. 2C and D). Similarly, anti-rPvMSP8 and anti-rPvMSP1-19 immune sera also had high IgG avidity responses with rPvMSP8+1 (mean, 89.15% and 86.20%, respectively) (Fig. 2E).

Validation of rPvMSP8, rPvMSP1-19, and rPvMSP8+1 polyclonal antibodies and immune sera. Considering that effective immune response could be induced in mice, immunofluorescence assays (IFAs) were conducted using anti-rPvMSP8, anti-rPvMSP1-19, or anti-rPvMSP8+1 polyclonal antibodies to investigate whether these antibodies could recognize the native proteins expressed on *P. vivax* merozoites. As expected, the antibodies of rPvMSP8+1, rPvMSP8, and rPvMSP1-19 could react with the native proteins on mature schizonts of *P. vivax* (Fig. 3A). Mouse immune sera and polyclonal antibodies were synchronously used to evaluate the specificity of these protein antigens via immunoblots and ELISA. As a positive control, anti-His antibody showed specific bands of protein antigens in lane 2. A single major band of rPvMSP8 could be detected with rPvMSP8- and rPvMSP8+1-specific antibodies (Fig. 3B, i). The same phenomenon was also observed for rPvMSP1-19 (Fig. 3B, ii), and rPvMSP8+1 could recognize anti-rPvMSP8 and anti-rPvMSP1-19 antibodies (Fig. 3B, iii). The results of ELISA showed that the control groups incubated only with PBS-immunized mouse serum did not present any reactivity with the protein antigens, whereas the group incubated with rPvMSP8+1-immunized mouse serum showed obvious reactivity with both rPvMSP8 and rPvMSP1-19 protein antigens (Fig. 3C). These findings may reflect the specific reactivity of anti-rPvMSP8+1 antibodies with the native proteins PvMSP8 and PvMSP1-19.

Humoral immune response analysis of rMSP8, rMSP1-19, and rMSP8+1 in *P. vivax* malaria patients. To examine if the MSP recombinant proteins could evaluate humoral immune response in patients with *P. vivax*, a protein array was performed to screen the presence of MSP antibodies in human serum samples against the purified proteins. Antibody responses against rPvMSP1-19 and rPvMSP8+1 were determined from 112 patients with *P. vivax* and 80 serum samples from uninfected healthy individuals. The prevalence of anti-rPvMSP8 and anti-rPvMSP1-19 antibodies showed that the sensitivities were 73.2% and 80.4% and the specificities were 96.3% and 93.8%, respectively (Table 1). As for rPvMSP8+1, the total IgG prevalence was 70.5% in sensitivity with 95% in specificity (Table 1). For rPvMSP1-19 and rPvMSP8+1, the serum samples from *P. vivax*-infected individuals exhibited a significantly higher mean fluorescence intensity (MFI) than those of uninfected healthy individuals (Fig. 4) ($P < 0.0001$). For rPvMSP8, a similar result was observed in our previous study on truncated PvMSP8 (21), which could partly represent rPvMSP8 in this study.

Recognition of MSP proteins in *P. cynomolgi* parasites. The *P. cynomolgi* Berok *in vitro* culture was used as a surrogate model for erythrocytic *P. vivax* studies. The MSP8 and MSP1-19 of *P. vivax* and *P. cynomolgi* showed high protein sequence similarity (90.97% of MSP8 and 86.52% of MSP1-19) (Fig. 5A). To assess cross-reactivity, an immunoblot analysis was performed against *P. cynomolgi* schizont lysates. All rPvMSP8-, rPvMSP1-19-, and rPvMSP8+1-specific antibodies could clearly recognize *P. cynomolgi* schizont lysates, but no specific band could be detected in uninfected naive red blood cell (RBC) lysates (Fig. 5B). Anti rPvMSP8, rPvMSP1-19, and rPvMSP8+1 antibodies showed merozoite surface labeling in a *P. cynomolgi* mature schizonts IFA assay (Fig. 5C). These results suggest that rPvMSP8-, rPvMSP1-19-, and rPvMSP8+1-specific antibodies cross-react with *P. cynomolgi* merozoites.

***In vitro* growth inhibition assay.** To determine the blocking activity of MSP antibodies against *P. cynomolgi*, rPvMSP8-, rPvMSP1-19-, or rPvMSP8+1-specific antibodies were serially diluted and incubated with the parasite culture for 96 h. Growth inhibition 50% inhibitory concentration (IC_{50}) values of 4.40, 1.59, and 0.94 μ g/ml were observed for rPvMSP8, rPvMSP1-19, or rPvMSP8+1 antibodies, respectively (Fig. 6). The

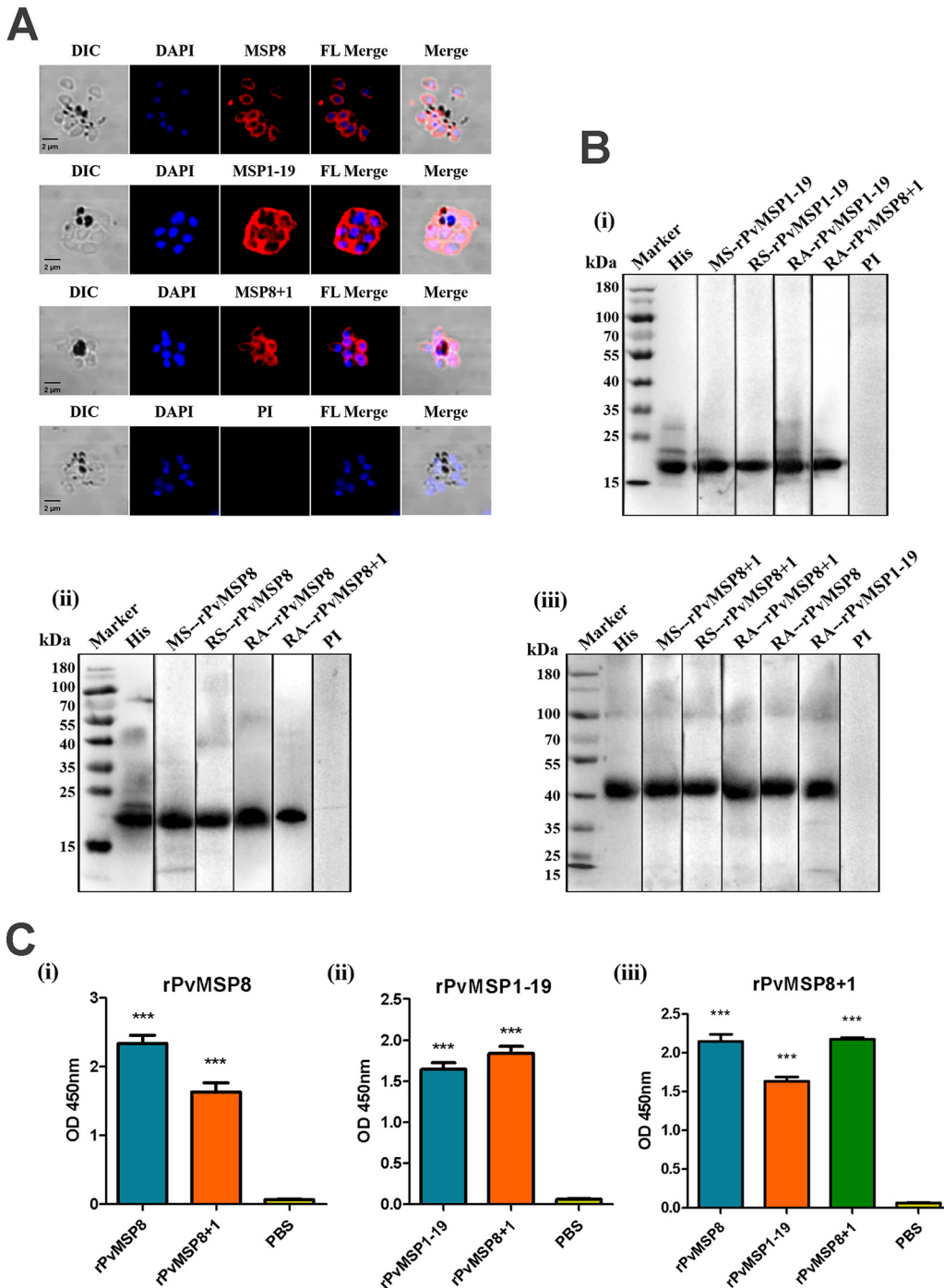


FIG 3 Production and validation of rPvMSP8, rPvMSP1-19, and rPvMSP8+1 polyclonal antibodies and immune serum samples. (A) Subcellular localization of rPvMSP8, rPvMSP1-19, and rPvMSP8+1 proteins. Schizont-stage parasites of *P. vivax* were labeled with rPvMSP8, rPvMSP1-19, and rPvMSP8+1 polyclonal antibodies (red) and preimmune rabbit serum. Nuclei were visualized with DAPI (blue) in merged images. PI, preimmune rabbit serum; DIC, differential interference contrast. (B) Western blot analysis of rPvMSP8, rPvMSP1-19, and rPvMSP8+1 using an anti-His antibody (His), mouse immune sera (MS), rabbit immune sera (RS), rabbit immune antibody (RA), and preimmune sera (PI). Molecular weight markers in kilodaltons (kDa) are indicated. (C) Cross-reaction of protein rPvMSP8 (i), rPvMSP1-19 (ii), or rPvMSP8+1 (iii) with sera from immune mice. PBS was used as negative control. A statistically significant difference was not observed.

preimmune serum was also diluted in the same manner as the tested antibodies and used as the negative control. For positive control, antibodies targeting Duffy antigen receptor for chemokines (DARC) Fy6 and FyB regions via Fy6 2C3 monoclonal and FyB polyclonal antibodies, respectively, were incubated with the *P. cynomolgi* continuous

TABLE 1 Prevalence (% positive), 95% confidence intervals, and mean fluorescence intensity of IgG responses to rPvMSP8, rPvMSP1-19, and rPvMSP8+1 in *P. vivax*-infected patient and uninfected healthy individual serum samples

Protein	No. of <i>P. vivax</i> infected patient samples			95% CI ^b (%)	MFI	No. of uninfected healthy samples			95% CI (%)	MFI	P value
	Positive ^a	Negative	Total no. (%)			Positive	Negative ^c	Total no. (%)			
rPvMSP8	82	30	112 (73.2)	64.3–80.6	17,867	3	77	80 (96.3)	89.6–98.7	1,363	<0.0001
rPvMSP1-19	90	22	112 (80.4)	73.1–87.7	15,572	5	75	80 (93.8)	88.4–99.0	3,346	<0.0001
rPvMSP8+1	79	33	112 (70.5)	62.0–78.9	17,611	4	76	80 (95.0)	92.6–97.4	6,427	<0.0001

^aSensitivity is the % positive in *P. vivax*-infected patient samples.

^bCI, confidence interval.

^cSpecificity is the % negative in uninfected healthy samples.

culture in macaque erythrocytes. We suspect that the IC₅₀ for Fy6 2C3 (13.14 μg/ml) to be higher than FyB (7.23 μg/ml) due to the slight difference in Fy6 amino acid residues between human (22FEDVW26) and macaque (22SEDLW26) DARC. Among the antibodies, the rPvMSP8+1 antibody showed the most effective inhibitory effect with the lowest IC₅₀ in all formulations (Table 2).

DISCUSSION

MSP remains a potential vaccine candidate against malaria due to its abundant protein expression in the asexual erythrocytic stages and its ability to confer disease protection in asymptomatic individuals. However, the inhibitory antibodies targeting *P. falciparum* MSP1-19 alone are effective with limited immunogenicity (18, 26). Similarly, the paralogue MSP8 in *P. vivax* induces potent immune responses in both humans and mouse models with limited immunogenicity (21). Interestingly, a recent study combined MSP8 and MSP1-19, specific to *P. yoelii*, and showed that the chimeric recombinant protein enhanced host immunogenicity and provided almost complete protection in mice infected with lethal *P. yoelii* 17XL malaria (22). Therefore, our study investigates *P. vivax* MSP8 as a fusion partner for MSP1-19 to assess its potentiality as a vaccine candidate for relapsing *P. vivax* malaria. In the present study, an antibody raised against the chimeric recombinant PvMSP8+1 protein was successfully developed and compared against antibodies to single rPvMSP8 or rPvMSP1-19 antigens. In

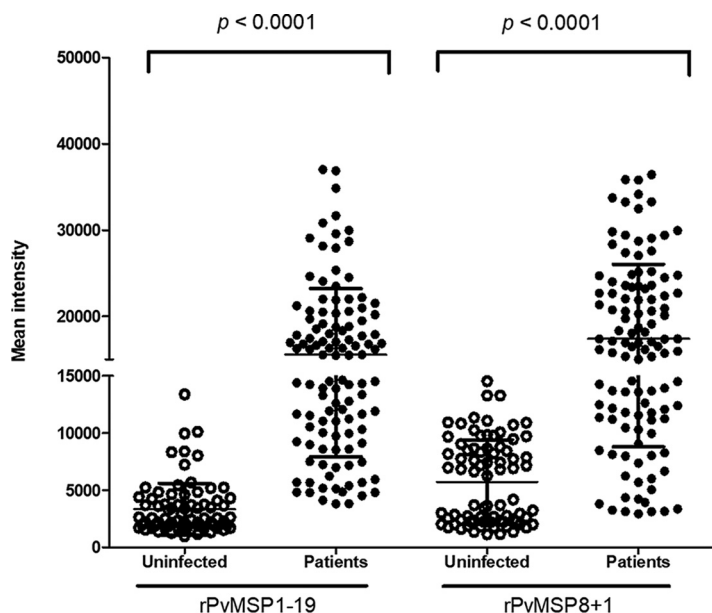


FIG 4 Total IgG responses to rPvMSP1-19 and rPvMSP8+1. rPvMSP1-19 and rPvMSP8+1 were probed with the serum samples of 112 *P. vivax* malaria patients and 80 healthy individuals from the ROK. Significant differences were observed between *P. vivax* patients and healthy individuals in the total prevalence of anti-rPvMSP1-19 and anti-rPvMSP8+1 IgG ($P < 0.0001$).

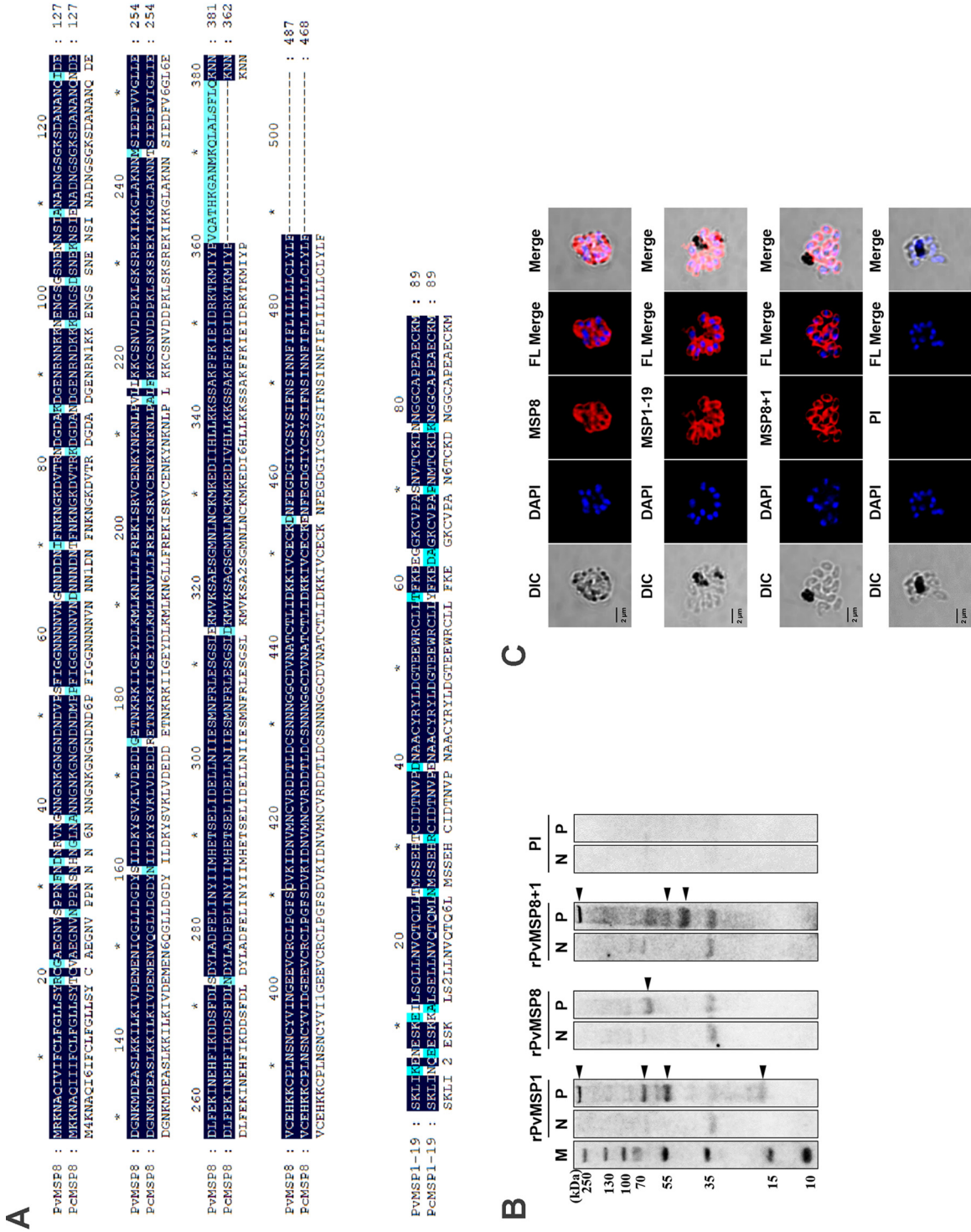


FIG 5 Cross-reactivity of rPvMSP8, rPvMSP1-19, or rPvMSP8+1 polyclonal antibodies with *P. cynomolgi*. (A) MSP8 and MSP1-19 amino acid sequence comparison between *P. vivax* and *P. cynomolgi*. The mazarin indicates identical sequence, and pale blue indicates diverse sequences. (B) Western blots showing rPvMSP8, rPvMSP1-19, or rPvMSP8+1 polyclonal antibodies reacting with *P. cynomolgi* parasite lysate. The clear multiple bands indicate processed naive PcMSP8 or PcMSP1-19. Preimmune serum samples were used as negative controls. Molecular weight is indicated to the left. M, molecular size marker. N, normal RBC lysate. P, *P. cynomolgi* lysate. (C) Reactivity observed by rPvMSP8, rPvMSP1-19, or rPvMSP8+1 polyclonal antibodies with *P. cynomolgi* merozoite at the schizont stage by IFAs. The mature schizont of *P. cynomolgi* was dually labeled with rPvMSP8, rPvMSP1-19, or rPvMSP8+1 polyclonal antibodies (red) and rabbit preimmune sera. Nuclei were visualized with DAPI (blue). Bar indicates 5 μm.

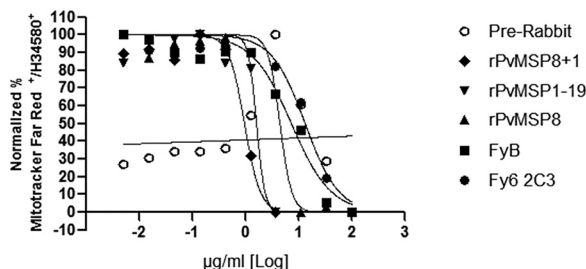


FIG 6 Invasion inhibition assay of rPvMSP8, rPvMSP1-19, or rPvMSP8+1 polyclonal antibodies with *P. cynomolgi* Berok. Data are shown as the proportion of live parasites stained. rPvMSP8, rPvMSP1-19, or rPvMSP8+1 polyclonal antibodies were used for invasion inhibition. Both Fy6 2C3 monoclonal antibody and FyB polyclonal antibody were used as positive controls. Preimmune sera were used as a negative control. The abscissa represents the antibody concentration.

mice immunized with rPvMSP8+1, an elevated antibody response was observed compared to that in mice immunized with either rPvMSP8 or rPvMSP1-19 alone. The antibodies purified from these mice recognized rPvMSP8, rPvMSP1-19, or rPvMSP8+1 in ELISA and the native protein on *P. vivax* and *P. cynomolgi* mature schizonts using IFA and Western blots. Furthermore, we examined the inhibition of these antibodies in *in vitro* growth inhibition assays using sister species *P. cynomolgi* and showed that antibodies raised against chimeric rPvMSP8+1 showed stronger growth inhibition than antibodies against rPvMSP8 or rPvMSP1-19 alone.

As important targets of human host immunity and potential vaccine candidates, merozoite surface antigens have been the subject of several recent studies. Recently, studies focused on multiple vaccine antigens derived from merozoite surface proteins have shown protective immunity against murine malaria (27, 28). To deeply evaluate the immune protection of PvMSP8 and PvMSP1-19 antigens, we first investigated whether their recombinant counterparts retained the native antigen specificity. The results of IFA, Western blot analysis, and ELISA showed that rPvMSP8+1 could be recognized by the immune sera of rPvMSP1-19 and rPvMSP8, and rPvMSP8+1-specific antibodies could also recognize native proteins expressed on *P. vivax* merozoites (Fig. 3). These results confirmed the successful construction of a highly specific multiple-protein antigen. Like PfMSP8 subcellular localization, PvMSP8 was found to be associated with the food vacuole in our previous study, whereas in the present study, PvMSP8 was located on the merozoite surface (13, 21, 29). This inconsistency may be because the rPvMSP8 that we used in the present study is only a region spanning 131 amino acid residues, while the earlier PvMSP8 that we used was almost the full-length fragment except for the removal of the signal peptide and GPI anchor. In comparing the immunogenicity of rPvMSP8+1 and a single antigen (rPvMSP1-19 or rPvMSP8), each recombinant could induce strong and equivalent antibody responses in mice. However, elevated endpoint titers were observed in mice immunized with rPvMSP8+1 compared with those of mice immunized with rPvMSP8 or rPvMSP1-19 (Fig. 2). This finding suggests that the theory of multiple-protein antigen (rPvMSP8+1) can address the limited immunogenicity observed with rPvMSP1-19. Merozoite surface proteins are

TABLE 2 IC₅₀ of rPvMSP8, rPvMSP1-19, and rPvMSP8+1 polyclonal antibodies with *P. cynomolgi* Berok using growth inhibition assay

Antibody	IC ₅₀ (µg/ml)
Fy6 2C3	13.14
FyB	7.239
rPvMSP8	4.402
rPvMSP1-19	1.598
rPvMSP8+1	0.9459
Preimmune	186,357,289

implicated in the invasion and destruction of erythrocytes; as membrane proteins, they are exposed to the host immune system and could, therefore, be recognized by the immune sera of infected patients from areas where malaria is endemic (8, 30). Naturally induced antibodies play important roles in eliminating blood-stage malaria parasites (31). In this study, the serum samples from *P. vivax*-exposed individuals also showed higher MFI than those from malaria-naïve subjects when probed against rPvMSP8, rPvMSP1-19, or rPvMSP8+1 (Fig. 4). These data confirm the antigenicity of rPvMSP8, rPvMSP1-19, and rPvMSP8+1 and may indirectly reflect their protection against malaria infection, as humoral immune responses may be partially associated with protection from infection of *P. vivax* parasites.

While the lack of a sustainable *in vitro* *P. vivax* culture limits the advancement of vaccines targeting *P. vivax* asexual blood-stage malaria, the recent reestablishment of an *in vitro* *P. cynomolgi* erythrocytic culture may provide some insights into various highly homologous surface proteins shared between the two species (24, 25). The *P. cynomolgi* MSP8 and MSP1-19 amino acid sequences are highly homologous to *P. vivax* at 90.97% and 86.52%, respectively. As such, the polyclonal antibodies raised against rPvMSP8, rPvMSP1-19, and chimeric rPvMSP8+1 antigens showed strong cross-reaction with *P. cynomolgi* schizont lysate (Fig. 5), supporting the use of *P. cynomolgi* as a surrogate model for *P. vivax*. When the antibodies were examined for their inhibition of parasite growth *in vitro*, antibodies against rPvMSP8+1 showed the lowest IC₅₀ required to block growth over 96 h (Fig. 6). The control antibodies applied in the growth inhibition assay include the monoclonal 2C3 Duffy antibody, which specifically recognizes the Fy6 domain on human Duffy antigen and the polyclonal FyB antibody (32, 33). Interestingly, the antibodies targeting the single rPvMSP8 and rPvMSP1-19 antigens achieved inhibition at a lower IC₅₀ than Fy6 2C3 and FyB antibodies (Fig. 6). This underpins the flexibility of the assay to examine antibodies targeting either merozoite ligands or host receptors and that the controls applied would hence provide variable assessment. Nonetheless, this result indicates that merozoite surface antigens play a significant role in initial attachment to host erythrocytes and suggests that the chimeric MSP8+1 is a promising vaccine candidate for the asexual erythrocytic stage of *P. vivax* malaria (34, 35). The mechanism of invasion inhibition by anti-MSP1-19 antibodies is not fully understood; however, MSP1-19 is composed almost entirely of two cysteine-rich EGF-like domains, which form reduction-sensitive epitopes and could be sterically hindered by invasion inhibitory monoclonal and polyclonal antibodies (36–38). Thus far, reports evaluating the ability of PvMSP8-specific antibodies to inhibit the invasion of erythrocytes by *Plasmodium* are lacking. The present study revealed the significant inhibition activity of antibodies directed against rPvMSP8, although the underlying mechanism is still unclear. Nevertheless, the potent immune responses of rPvMSP8 and rPvMSP1-19 in humans and mouse models and their significant inhibition activity make them suitable fusion partners to improve vaccine efficacy. As expected, anti-rPvMSP8+1-specific antibodies showed the most effective inhibition activity *in vitro*, showing the superiority of a chimeric protein vaccine compared with single antigen components (Table 2). This finding is similar to the superiority of chimeric PfMSP1/8, whose specific antibody could potentially inhibit the *in vitro* growth of blood-stage parasites (23). Overall, our data indicated the inhibitory role of antibodies to rPvMSP8, rPvMSP1-19, and rPvMSP8+1 on *P. cynomolgi* merozoite invasion to macaque erythrocytes.

From an immunogenicity perspective, the findings of the present study raised the possibility that protective epitopes of the native protein may be represented in recombinant constructs of MSP8 and MSP1-19. The antibodies that were raised based on these constructs could limit *P. cynomolgi* growth *in vitro* and simultaneously showed strong cross-reaction to schizont lysates via Western blot analysis. It would thus be of interest to determine whether the antibodies would similarly confer strong inhibition in short-term *in vitro* *P. vivax* invasion inhibition assays or applied *in vivo* using monkeys challenged with *P. cynomolgi* infection (39, 40). One of the rationales

for blood-stage vaccine development is based on the premise that the host immune response would be enhanced to inhibit multiplicity of merozoite invasion and growth, thereby reducing parasitemia and morbidity (41). Thus, this attempt is highly desirable for the development of a vaccine against *P. vivax*. Previous studies have demonstrated that CD4⁺ T helper cells are essential for the introduction of anti-MSP1-19 antibodies and that MSP1-specific CD8⁺ T cells have an effect on exoerythrocytic-stage development (42, 43). The recombinant modular chimera PyRMC-MSP1-19 could also elicit high antiparasite antibody titers and robust protection against hyperparasitemia and malarial anemia (43). However, the IgG titer intensity in the rPvMSP8+1-immunized group could not be compared with that of the rPvMSP8- or rPvMSP1-19-immunized group in this study. Therefore, evaluating the critical role of rPvMSP8+1-specific T cells in protective immunity will be a research priority in the future. In addition, another challenge facing the development of this subunit vaccine that remains to be addressed is the polymorphism of the C-terminal 42-kDa region of PvMSP1 (44). Previous studies have demonstrated the allelic variation in the 33-kDa encoding region, while the C-terminal 19-kDa fragment (PvMSP1-19) is highly conserved with only one substitution at position 1709 (K/E) (44–46). Although there are two allelic forms of PvMSP1-19, previous seroepidemiological study has shown that the conserved epitopes in this region are the targets of antibody response (47). Also, another approach to further address this issue of polymorphism could be immunization with a combined formulation containing multiple alleles of PvMSP1-19.

In summary, we report the design and expression of a recombinant chimeric protein that includes single antigens derived from *P. vivax* MSP8 and MSP1-19. The chimeric rPvMSP8+1 protein exhibited antigenic characteristics similar to those of the original parental proteins. The recombinant PvMSP8+1 showed superior effects in inducing immune response and parasite growth inhibitory ability compared with those of the individual components of the protein. Although the protective effects of multifunctional CD4⁺ and CD8⁺ T cells induced by immunization were not elucidated, the findings from this study provide a basis for *in vivo* testing in nonhuman primates to evaluate the vaccine potential of chimeric rPvMSP8+1.

MATERIALS AND METHODS

Ethics. All experiments were performed in accordance with relevant guidelines and regulations and all experimental protocols involving human samples approved by the ethics committees of the Kangwon National University Hospital in the Republic of Korea (ROK) (KWNUIRB-2016-04-005), the Faculty of Tropical Medicine, Mahidol University in Thailand (MUIRB2012/079.2408), and the Department of Medical Research, Republic of the Union of Myanmar (approval no. 52/Ethics, 2012). This study was approved by the Institutional Review Board at Kangwon National University Hospital. Written informed consent was obtained from all subjects and their guardians, and the mouse trial was approved by the Animal Ethics Committee of Jiangnan University (JN. no. 20180615t0900930 [100]).

Animals. *Macaca fascicularis* (cynomolgus monkeys) were maintained at Monash Animal Research Platform (MARF), Gippsland, Australia. All animals were housed in accordance with the Australian Code of Practice and the Laboratory Animals Code of Practice. Blood collection from cynomolgus monkeys followed standard operating procedures within MARF. All import and export permits were approved by the Convention on International Trade in Endangered Species of Wild Fauna and Flora. All import declarations were approved by the Ministry of Primary Industries, New Zealand.

Parasite culture. *P. cynomolgi* Berok strain was cultured in RPMI 1640 medium supplemented with GlutaMax containing 30 mM HEPES, 0.2% (wt/vol) D-glucose, and 200 μM hypoxanthine supplemented with 20% (vol/vol) heat-inactivated *M. fascicularis* serum. The parasite culture was maintained at 5% hematocrit and 37°C in a sealed chamber filled with trimix gas (5% O₂, 5% CO₂, and the rest with N₂).

Study sites and sample collection. The blood samples were collected in three areas where malaria is endemic in the Republic of Korea (ROK) (*n* = 11), Thailand (*n* = 7), and Myanmar (*n* = 12) from 2014 to 2016, 2013, and 2012, respectively. The healthy individual serum samples were collected from children under 10 years old with no malaria history in local hospitals of areas where malaria is not endemic in the ROK. For the determination of immunoglobulin G (IgG) levels, a total of 112 serum samples were collected from malaria febrile patients with symptoms and positive *P. vivax* density by microscopic examination (40,000 to 260,000 parasites/μl) from Tengchong county, an area at the China-Myanmar border of the Yunnan province in 2016. In addition, 80 serum samples of healthy individuals that tested negative for *P. vivax* malaria by microscopy were collected in areas of China where malaria is not endemic (Wuxi city, Jiangsu province). The study was approved by the Ethics Committee of the National Institute of Parasitic Diseases (NIPD), China CDC.

Production and purification of recombinant proteins. Gene sequences of *pvmSP8* and *pvmSP1* were obtained from the PlasmoDB website (<https://plasmodb.org/plasmo/app>; accession no. PVX_097625 and PVX_099980). The PvMSP8 partial peptides (aa 260 to 390) were intercepted in accordance with our previous study (21). Both sequences of PvMSP8 and PvMSP1-19 were from the Sal-1 strain of *P. vivax*, and *pvmSP8*, *pvmSP1-19*, and *pvmSP8+1* were generated by DNA synthesis (Genewiz Bio, Suzhou, China). The gene inserts were then subcloned into the BamHI and XhoI sites of a pET-30a expression vector (YouLong Bio, Shanghai, China). This vector adds thioredoxin and six-histidine tags at the N- and C-terminal ends, enabling easier purification and immunodetection using polyclonal antibodies against the six-histidine tag. The vector for rPvMSP8+1 was finally replaced with pET-32a (YouLong Bio, Shanghai, China), which also contains six-histidine tags. *Escherichia coli* cells were used as the expression host. The proteins rPvMSP8, rPvMSP1-19, and rPvMSP8+1 were purified using a Ni-Sephareose column under nondenaturing conditions by YouLong Bio, Shanghai, China.

Animal immune sera and purification of IgG. rPvMSP8, rPvMSP1-19, and rPvMSP8+1 were used for raising immune sera and antibodies. Groups of five female BALB/c mice (5 to 6 weeks of age) were injected intraperitoneally with 25 μ g of rPvMSP8, rPvMSP1-19, rPvMSP8+1, or phosphate-buffered saline (PBS) with Freund's complete adjuvant (Sigma) as described previously (48). Three and 6 weeks after the priming immunization, the same amount of antigen with Freund's incomplete adjuvant (Sigma) was boosted, and the serum of each mouse was collected at days 0, 7, 14, 28, 35, and 49 postimmunization. Control mice were immunized with a mixture of PBS and adjuvant. Meanwhile, polyclonal rabbit antisera and IgG fractions were generated by YouLong Bio, Shanghai, China. Briefly, 2-month-old New Zealand rabbits were immunized with 500 μ g of purified rPvMSP8, rPvMSP1-19, or rPvMSP8+1 plus Freund's complete adjuvant (Sigma) followed by 500 μ g of Freund's incomplete adjuvant (Sigma). All immunizations were conducted three times at 3-week intervals, and the antisera were collected 2 weeks after the final booster. Each antiserum was purified by protein A affinity chromatography after precipitation with ammonium sulfate.

Enzyme-linked immunosorbent assay. Antigen-specific antibody responses induced by immunization with rPvMSP8, rPvMSP1-19, or rPvMSP8+1 were evaluated by ELISA. Briefly, ELISA plates were coated with 100 ng per well of rPvMSP8, rPvMSP1-19, or rPvMSP8+1 diluted in coating buffer (15 mM Na₂CO₃ and 35 mM NaHCO₃ in 1,000 ml ultrapure water) and incubated overnight at 4°C. Antigen-coated plates were washed and then blocked with Tris-buffered saline (TBS) containing 0.1% Tween 20 (TBST) containing 5% skim milk at room temperature for 2 h. Two-fold serial dilutions of mouse serum samples starting at 1:10,000 were added to antigen-coated wells and incubated for 2 h at room temperature. Bound antibodies were detected with tetramethylbenzidine solution (Sigma) after being incubated with horseradish peroxidase-conjugated goat anti-mouse IgG antibody (Sigma). For each dilution, the absorbance was then measured at 450 nm (A_{450}). Antibody responses to rPvMSP8, rPvMSP1-19, or rPvMSP8+1 at 0, 7, 14, 28, 35, and 49 days after primary immunization were evaluated as described above, except that the mouse serum samples were diluted at 1:10,000.

The avidity of anti-rPvMSP8, rPvMSP1-19, or rPvMSP8+1 IgG antibodies was estimated as described previously (49). Briefly, ELISA testing was performed in duplicate plates. After dilution of the serum samples (1:10,000) and incubation for 90 min, one of the plates was washed three times with TBST, and the other plate was washed three times with dissociation buffer containing TBST with 6 M urea. Thereafter, the plates were washed once with TBST buffer. Incubation with a secondary antibody, washing, and development of the enzyme reaction were performed as described above. The avidity index (AI) for each sample was calculated as follows: AI = (optical density at 450 nm [OD_{450}] of a sample treated with 6 M urea/ OD_{450} of a sample not treated with 6 M urea) \times 100%.

Serum screening using protein arrays. Amine-coated slides were prepared as described previously (50, 51). Serum samples from 112 patients infected with *P. vivax* malaria and 80 healthy individuals were tested against rPvMSP1-19 and rPvMSP8+1 using protein arrays. A series of double dilutions was developed to optimize the coating concentration (0.1 to 200 μ g/ml) of recombinant proteins. The purified rPvMSP1-19, rPvMSP8+1, or PBS (100 μ g/ml) was spotted in duplicate onto array slides and incubated for 2 h at 37°C. Each slide was blocked with 1 μ l blocking buffer (5% bovine serum albumin in PBS with 0.1% Tween 20 [PBST]) and incubated for 1 h at 37°C. The chips were preabsorbed against wheat germ lysate (1:100 dilution) to block anti-wheat germ antibodies and then probed with serum samples of human malaria patients or healthy individuals (1:200 dilution). Alexa Fluor 546 goat anti-human IgG (10 μ g/ml, Sigma) in PBST was used to detect antibodies, and the antibodies were scanned in a fluorescence scanner (ScanArray Express, Boston, USA). Fluorescence intensities of array spots were quantified by the fixed-circle method using ScanArray Express software (version 4.0; PerkinElmer). The cutoff value was equal to the mean plus 2 standard deviations of the mean intensity of 80 negative samples.

Indirect immunofluorescence assay. Enriched schizont-stage parasites were purified by Percoll gradient centrifugation, spotted onto a multiwell slide, fixed in ice-cold acetone for 3 min, air-dried, and stored at -80°C. Before use, the slides were thawed on silica gel blue (Samchun Chemical, Pyeongtaek, ROK), and nonspecific binding sites were blocked with PBS containing 5% skim milk at 37°C for 30 min. The slides were incubated with 1:100 diluted primary antibodies, rabbit anti-rPvMSP8, rabbit anti-rPvMSP1-19, or rabbit anti-rPvMSP8+1, at 37°C for 1 h. After washing three times with cold PBS, the slides were stained with Alexa Fluor 546-conjugated goat anti-rabbit IgG secondary antibody (Invitrogen, Carlsbad, USA), and the nuclei were stained with 4',6-diamidino-2-phenylindole (DAPI) (Invitrogen) at 37°C for 30 min. The slides were mounted with coverslips in ProLong Gold Antifade reagent (Invitrogen) and visualized under oil immersion using a confocal laser scanning FV200 microscope (Olympus, Tokyo, Japan) equipped with 20 \times dry and 60 \times oil objectives. Images were captured with

EV10-ASW version 3.0 viewer software (Olympus) and prepared for publication with Adobe Photoshop CS5 (Adobe Systems, San Jose, CA, USA).

SDS-PAGE and Western blot analysis. Protein expression and purity were verified by Coomassie blue staining analysis following SDS-PAGE on 10% and/or 12% gels run under both reducing and non-reducing conditions. Immunoblots were probed with an anti-His antibody (Sigma). Following electrophoresis, the proteins were blotted onto polyvinylidene difluoride (PVDF) membranes and incubated with blocking buffer (5% skim milk in PBST) for 2 h at room temperature. The membranes were then incubated overnight at 4°C with anti-His antibody (Sigma), and secondary goat anti-mouse (Sigma) antibodies were used to detect His-tagged recombinant proteins. Results were visualized using a chemiluminescence detection assay (ECL; New Cell and Molecular Biotech, China), and images were merged using ImageJ software. For immune serum and antibody specificity, mouse immune sera, rabbit immune sera, and antibodies against rPvMSP8, rPvMSP1-19, or rPvMSP8+1 were used as primary antibodies for incubation. The following steps were performed as described above.

To test whether specific antibodies against rPvMSP8, rPvMSP1-19, or rPvMSP8+1 could be recognized by *P. cynomolgi*-infected erythrocyte lysates or monkey healthy erythrocyte lysates, *P. cynomolgi*-infected erythrocyte lysates were collected and mixed with SDS sample buffer for proper separation by SDS-PAGE. After immunoblots were transferred to PVDF membranes, antibodies against rPvMSP8, rPvMSP1-19, or rPvMSP8+1 were used as primary antibodies for incubation. The following steps were performed as described above.

P. cynomolgi growth inhibition assay. A presynchronized culture was adjusted to 1% hematocrit and 0.5% parasitemia and then plated at 0.63 ml/well in a 96-well round-bottomed plate. Antibodies were prepared by serial dilution at 1 mg/ml (well no. 1). All antibodies were prepared by 3-fold serial dilution with *P. cynomolgi*-based medium for 10 concentration points. Approximately 7 μ l of antibodies was added in duplicate to parasites. At 48 h postincubation, each well was refreshed with 7 μ l of complete growth medium. At 96 h postincubation, 20 μ l of culture from each well was aliquoted into a fresh round-bottomed plate, stained with 8 μ M Hoechst 34580 and 150 nM MitoTracker deep red FM molecular probes, and acquired on a Canto II flow cytometer (Becton, Dickinson). The plates were incubated with dyes for 20 min away from light at room temperature, washed twice with 200 μ l PBS each time, and transferred to 3-ml round-bottom polystyrene tubes (Becton, Dickinson) for acquisition. Monoclonal antibody Fy6 2C3 (murine anti-Fy6) and polyclonal antibody FyB were used as invasion inhibition controls. Data were analyzed using FlowJo software (Tree Star Inc.) where single cells were gated. Values indicated in double positive population Hoechst 34580⁺/MitoTracker Deep Red⁺ were exported to Excel software and analyzed using FlowJo software.

Statistical analysis. The correlation between antibody reactivity to different concentrations of recombinant proteins and duplicate spots of protein arrays was observed using GraphPad Prism software version 5.0 and PASW Statistics 18.0. Sensitivity and specificity were measured by the proportion of patients who had a positive test result and that of healthy individuals who had a negative test result, respectively. The significance of differences in mean fluorescence intensity (MFI) values between every two groups was determined using the Mann-Whitney U test.

ACKNOWLEDGMENTS

We are grateful to Yves Colin, Institut National de la Transfusion Sanguine, Paris, France for providing the 2C3 monoclonal antibody.

This work was financially supported by the National Natural Science Foundation of China under grants (81871681), by the Fundamental Research Funds for the Central Universities funded by the Ministry of Education of China under grants (JUSRP51710A), by the Bill and Melinda Gates Foundation under grants (OPP1161962), by the National First-Class Discipline Program of Food Science and Technology under grants (JUFSTR20180101), by the China Postdoctoral Science Foundation (2018M642171), by the Jiangsu Postdoctoral Sustentation Fund (2018K236C), and by the Scientific Research Project of Public Health Research Center of Jiangnan University (1286066903190040). This research was also supported by the Royal Society New Zealand Marsden Fund (UOO1710) and 2018 Deans' Bequest, University of Otago, School of Medical Sciences.

REFERENCES

- World Health Organization. 2019. World malaria report 2019. World Health Organization, Geneva, Switzerland.
- Feng J, Zhang L, Zhang S, Xia Z, Zhou S. 2017. Malaria epidemiological characteristics in China, 2005–2015. *China Tropical Medicine* 17:325–335.
- Zhang L, Feng J, Zhang S, Xia Z, Zhou S. 2018. The progress of national malaria elimination and epidemiological characteristics of malaria in China in 2017. *Chin J Parasitol Parasit Dis* 36:201–209.
- Zhang L, Feng J, Xia Z, Zhou S. 2020. Epidemiological characteristics of malaria and progress on its elimination in China in 2019. *Chin J Parasitol Parasit Dis* 38:1–5.
- Price RN, von Seidlein L, Valecha N, Nosten F, Baird JK, White NJ. 2014. Global extent of chloroquine-resistant *Plasmodium vivax*: a systematic review and meta-analysis. *Lancet Infect Dis* 14:982–991. [https://doi.org/10.1016/S1473-3099\(14\)70855-2](https://doi.org/10.1016/S1473-3099(14)70855-2).
- Bennett JW, Yadava A, Tosh D, Sattabongkot J, Komisar J, Ware LA, McCarthy WF, Cowden JJ, Regules J, Spring MD, Paolino K, Hartzell JD, Cummings JF, Richie TL, Lumsden J, Kamau E, Murphy J, Lee C, Parekh F, Birkett A, Cohen J, Ballou WR, Polhemus ME, Vanloubbeeck YF, Vekemans J, Ockenhouse CF. 2016. Phase 1/2a trial of *Plasmodium vivax* malaria vaccine candidate VMP001/AS01B in malaria-naive adults: safety,

- immunogenicity, and efficacy. *PLoS Negl Trop Dis* 10:e0004423. <https://doi.org/10.1371/journal.pntd.0004423>.
7. Herrera S, Bonelo A, Perlaza BL, Fernandez OL, Victoria L, Lenis AM, Soto L, Hurtado H, Acuna LM, Velez JD, Palacios R, Chen-Mok M, Corradin G, Arevalo-Herrera M. 2005. Safety and elicitation of humoral and cellular responses in Colombian malaria-naïve volunteers by a *Plasmodium vivax* circumsporozoite protein-derived synthetic vaccine. *Am J Trop Med Hyg* 73:3–9. <https://doi.org/10.4269/ajtmh.2005.73.3>.
 8. Reeder JC, Wapling J, Mueller I, Siba PM, Barry AE. 2011. Population genetic analysis of the *Plasmodium falciparum* 6-cys protein Pf38 in Papua New Guinea reveals domain-specific balancing selection. *Malar J* 10:126. <https://doi.org/10.1186/1475-2875-10-126>.
 9. Holder AA, Blackman MJ, Borre M, Burghaus PA, Chappel JA, Keen JK, Ling IT, Ogun SA, Owen CA, Sinha KA. 1994. Malaria parasites and erythrocyte invasion. *Biochem Soc Trans* 22:291–295. <https://doi.org/10.1042/bst0220291>.
 10. Smythe JA, Coppel RL, Brown GV, Ramasamy R, Kemp DJ, Anders RF. 1988. Identification of two integral membrane proteins of *Plasmodium falciparum*. *Proc Natl Acad Sci U S A* 85:5195–5199. <https://doi.org/10.1073/pnas.85.14.5195>.
 11. Marshall VM, Silva A, Foley M, Cranmer S, Wang L, McColl DJ, Kemp DJ, Coppel RL. 1997. A second merozoite surface protein (MSP-4) of *Plasmodium falciparum* that contains an epidermal growth factor-like domain. *Infect Immun* 65:4460–4467. <https://doi.org/10.1128/IAI.65.11.4460-4467.1997>.
 12. Marshall VM, Tieqiao W, Coppel RL. 1998. Close linkage of three merozoite surface protein genes on chromosome 2 of *Plasmodium falciparum*. *Mol Biochem Parasitol* 94:13–25. [https://doi.org/10.1016/s0166-6851\(98\)00045-0](https://doi.org/10.1016/s0166-6851(98)00045-0).
 13. Black CG, Wu T, Wang L, Hibbs AR, Coppel RL. 2001. Merozoite surface protein 8 of *Plasmodium falciparum* contains two epidermal growth factor-like domains. *Mol Biochem Parasitol* 114:217–226. [https://doi.org/10.1016/s0166-6851\(01\)00265-1](https://doi.org/10.1016/s0166-6851(01)00265-1).
 14. Black CG, Wang L, Wu T, Coppel RL. 2003. Apical location of a novel EGF-like domain-containing protein of *Plasmodium falciparum*. *Mol Biochem Parasitol* 127:59–68. [https://doi.org/10.1016/s0166-6851\(02\)00308-0](https://doi.org/10.1016/s0166-6851(02)00308-0).
 15. Blackman MJ, Ling IT, Nicholls SC, Holder AA. 1991. Proteolytic processing of the *Plasmodium falciparum* merozoite surface protein-1 produces a membrane-bound fragment containing two epidermal growth factor-like domains. *Mol Biochem Parasitol* 49:29–33. [https://doi.org/10.1016/0166-6851\(91\)90127-r](https://doi.org/10.1016/0166-6851(91)90127-r).
 16. Blackman MJ, Heidrich HG, Donachie S, McBride JS, Holder AA. 1990. A single fragment of a malaria merozoite surface protein remains on the parasite during red cell invasion and is the target of invasion-inhibiting antibodies. *J Exp Med* 172:379–382. <https://doi.org/10.1084/jem.172.1.379>.
 17. Siddiqui WA, Tam LQ, Kramer KJ, Hui GS, Case SE, Yamaga KM, Chang SP, Chan EB, Kan SC. 1987. Merozoite surface coat precursor protein completely protects Aotus monkeys against *Plasmodium falciparum* malaria. *Proc Natl Acad Sci U S A* 84:3014–3018. <https://doi.org/10.1073/pnas.84.9.3014>.
 18. Egan A, Waterfall M, Pinder M, Holder A, Riley E. 1997. Characterization of human T- and B-cell epitopes in the C terminus of *Plasmodium falciparum* merozoite surface protein 1: evidence for poor T-cell recognition of polypeptides with numerous disulfide bonds. *Infect Immun* 65:3024–3031. <https://doi.org/10.1128/IAI.65.8.3024-3031.1997>.
 19. Burns JM, Jr, Belk CC, Dunn PD. 2000. A protective glycosylphosphatidylinositol-anchored membrane protein of *Plasmodium yoelii* trophozoites and merozoites contains two epidermal growth factor-like domains. *Infect Immun* 68:6189–6195. <https://doi.org/10.1128/68.11.6189-6195.2000>.
 20. Puentes A, Garcia J, Ocampo M, Rodriguez L, Vera R, Curtidor H, Lopez R, Suarez J, Valbuena J, Vanegas M, Guzman F, Tovar D, Patarroyo ME. 2003. *P. falciparum*: merozoite surface protein-8 peptides bind specifically to human erythrocytes. *Peptides* 24:1015–1023. [https://doi.org/10.1016/s0196-9781\(03\)00185-2](https://doi.org/10.1016/s0196-9781(03)00185-2).
 21. Cheng Y, Wang B, Changrob S, Han JH, Sattabongkot J, Ha KS, Chootong P, Lu F, Cao J, Nyunt MH, Park WS, Hong SH, Lim CS, Tsuboi T, Han ET. 2017. Naturally acquired humoral and cellular immune responses to *Plasmodium vivax* merozoite surface protein 8 in patients with *P. vivax* infection. *Malar J* 16:211. <https://doi.org/10.1186/s12936-017-1837-5>.
 22. Shi Q, Lynch MM, Romero M, Burns JM, Jr. 2007. Enhanced protection against malaria by a chimeric merozoite surface protein vaccine. *Infect Immun* 75:1349–1358. <https://doi.org/10.1128/IAI.01467-06>.
 23. Alaro JR, Partridge A, Miura K, Diouf A, Lopez AM, Angov E, Long CA, Burns JM, Jr. 2013. A chimeric *Plasmodium falciparum* merozoite surface protein vaccine induces high titers of parasite growth inhibitory antibodies. *Infect Immun* 81:3843–3854. <https://doi.org/10.1128/IAI.00522-13>.
 24. Nguyen-Dinh P, Gardner AL, Campbell CC, Skinner JC, Collins WE. 1981. Cultivation *in vitro* of the vivax-type malaria parasite *Plasmodium cynomolgi*. *Science* 212:1146–1148. <https://doi.org/10.1126/science.7233207>.
 25. Tachibana S, Sullivan SA, Kawai S, Nakamura S, Kim HR, Goto N, Arisue N, Palacpac NM, Honma H, Yagi M, Tougan T, Katakai Y, Kaneko O, Mita T, Kita K, Yasutomi Y, Sutton PL, Shakhbatyan R, Horii T, Yasunaga T, Barnwell JW, Escalante AA, Carlton JM, Tanabe K. 2012. *Plasmodium cynomolgi* genome sequences provide insight into *Plasmodium vivax* and the monkey malaria clade. *Nat Genet* 44:1051–1055. <https://doi.org/10.1038/ng.2375>.
 26. Egan AF, Burghaus P, Druilhe P, Holder AA, Riley EM. 1999. Human antibodies to the 19 kDa C-terminal fragment of *Plasmodium falciparum* merozoite surface protein 1 inhibit parasite growth *in vitro*. *Parasite Immunol* 21:133–139. <https://doi.org/10.1046/j.1365-3024.1999.00209.x>.
 27. Alaro JR, Angov E, Lopez AM, Zhou H, Long CA, Burns JM, Jr. 2012. Evaluation of the immunogenicity and vaccine potential of recombinant *Plasmodium falciparum* merozoite surface protein 8. *Infect Immun* 80:2473–2484. <https://doi.org/10.1128/IAI.00211-12>.
 28. Singh B, Cabrera-Mora M, Jiang J, Moreno A. 2012. A hybrid multistage protein vaccine induces protective immunity against murine malaria. *Infect Immun* 80:1491–1501. <https://doi.org/10.1128/IAI.05980-11>.
 29. Drew DR, Sanders PR, Crabb BS. 2005. *Plasmodium falciparum* merozoite surface protein 8 is a ring-stage membrane protein that localizes to the parasitophorous vacuole of infected erythrocytes. *Infect Immun* 73:3912–3922. <https://doi.org/10.1128/IAI.73.7.3912-3922.2005>.
 30. Sanders PR, Gilson PR, Cantin GT, Greenbaum DC, Nebl T, Carucci DJ, McConville MJ, Schofield L, Hodder AN, Yates JR, III, Crabb BS. 2005. Distinct protein classes including novel merozoite surface antigens in Raft-like membranes of *Plasmodium falciparum*. *J Biol Chem* 280:40169–40176. <https://doi.org/10.1074/jbc.M509631200>.
 31. Langhorne J, Ndungu FM, Sponaas AM, Marsh K. 2008. Immunity to malaria: more questions than answers. *Nat Immunol* 9:725–732. <https://doi.org/10.1038/nif.205>.
 32. Cho JS, Russell B, Kosaisavee V, Zhang R, Colin Y, Bertrand O, Chandramohanadas R, Chu CS, Nosten F, Renia L, Malleret B. 2016. Unambiguous determination of *Plasmodium vivax* reticulocyte invasion by flow cytometry. *Int J Parasitol* 46:31–39. <https://doi.org/10.1016/j.ijpara.2015.08.003>.
 33. Muh F, Ahmed MA, Han JH, Nyunt MH, Lee SK, Lau YL, Kaneko O, Han ET. 2018. Cross-species analysis of apical asparagine-rich protein of *Plasmodium vivax* and *Plasmodium knowlesi*. *Sci Rep* 8:5781. <https://doi.org/10.1038/s41598-018-23728-1>.
 34. Beeson JG, Drew DR, Boyle MJ, Feng G, Fowkes FJ, Richards JS. 2016. Merozoite surface proteins in red blood cell invasion, immunity and vaccines against malaria. *FEMS Microbiol Rev* 40:343–372. <https://doi.org/10.1093/femsre/fuw001>.
 35. Cowman AF, Crabb BS. 2006. Invasion of red blood cells by malaria parasites. *Cell* 124:755–766. <https://doi.org/10.1016/j.cell.2006.02.006>.
 36. Morgan WD, Birdsall B, Frenkiel TA, Gradwell MG, Burghaus PA, Syed SE, Uthairipull C, Holder AA, Feeney J. 1999. Structure of an EGF module pair from the *Plasmodium falciparum* merozoite surface protein 1. *J Mol Biol* 289:113–122. <https://doi.org/10.1006/jmbi.1999.2753>.
 37. Chappel JA, Holder AA. 1993. Monoclonal antibodies that inhibit *Plasmodium falciparum* invasion *in vitro* recognise the first growth factor-like domain of merozoite surface protein-1. *Mol Biochem Parasitol* 60:303–311. [https://doi.org/10.1016/0166-6851\(93\)90141-j](https://doi.org/10.1016/0166-6851(93)90141-j).
 38. O'Donnell RA, Saul A, Cowman AF, Crabb BS. 2000. Functional conservation of the malaria vaccine antigen MSP-1₁₉ across distantly related *Plasmodium* species. *Nat Med* 6:91–95. <https://doi.org/10.1038/71595>.
 39. Stowers AW, Cioce V, Shimp RL, Lawson M, Hui G, Muratova O, Kaslow DC, Robinson R, Long CA, Miller LH. 2001. Efficacy of two alternate vaccines based on *Plasmodium falciparum* merozoite surface protein 1 in an Aotus challenge trial. *Infect Immun* 69:1536–1546. <https://doi.org/10.1128/IAI.69.3.1536-1546.2001>.
 40. Stowers AW, Chen LH, Zhang Y, Kennedy MC, Zou L, Lambert L, Rice TJ, Kaslow DC, Saul A, Long CA, Meade H, Miller LH. 2002. A recombinant vaccine expressed in the milk of transgenic mice protects Aotus monkeys from a lethal challenge with *Plasmodium falciparum*. *Proc Natl Acad Sci U S A* 99:339–344. <https://doi.org/10.1073/pnas.012590199>.
 41. Good MF. 2001. Towards a blood-stage vaccine for malaria: are we

- following all the leads? Nat Rev Immunol 1:117–125. <https://doi.org/10.1038/35100540>.
42. Draper SJ, Goodman AL, Biswas S, Forbes EK, Moore AC, Gilbert SC, Hill AV. 2009. Recombinant viral vaccines expressing merozoite surface protein-1 induce antibody- and T cell-mediated multistage protection against malaria. Cell Host Microbe 5:95–105. <https://doi.org/10.1016/j.chom.2008.12.004>.
 43. Singh B, Cabrera-Mora M, Jiang J, Galinski M, Moreno A. 2010. Genetic linkage of autologous T cell epitopes in a chimeric recombinant construct improves anti-parasite and anti-disease protective effect of a malaria vaccine candidate. Vaccine 28:2580–2592. <https://doi.org/10.1016/j.vaccine.2010.01.019>.
 44. Putaporntip C, Jongwutiwes S, Seethamchai S, Kanbara H, Tanabe K. 2000. Intragenic recombination in the 3' portion of the merozoite surface protein 1 gene of *Plasmodium vivax*. Mol Biochem Parasitol 109:111–119. [https://doi.org/10.1016/s0166-6851\(00\)00238-3](https://doi.org/10.1016/s0166-6851(00)00238-3).
 45. Pasay MC, Cheng Q, Rzepczyk C, Saul A. 1995. Dimorphism of the C terminus of the *Plasmodium vivax* merozoite surface protein 1. Mol Biochem Parasitol 70:217–219. [https://doi.org/10.1016/0166-6851\(95\)00015-5](https://doi.org/10.1016/0166-6851(95)00015-5).
 46. Soares IS, Barnwell JW, Ferreira MU, Gomes Da Cunha M, Laurino JP, Castilho BA, Rodrigues MM. 1999. A *Plasmodium vivax* vaccine candidate displays limited allele polymorphism, which does not restrict recognition by antibodies. Mol Med 5:459–470. <https://doi.org/10.1007/BF03403539>.
 47. Soares IS, Oliveira SG, Souza JM, Rodrigues MM. 1999. Antibody response to the N and C-terminal regions of the *Plasmodium vivax* merozoite surface protein 1 in individuals living in an area of exclusive transmission of *P. vivax* malaria in the north of Brazil. Acta Trop 72:13–24. [https://doi.org/10.1016/S0001-706X\(98\)00078-3](https://doi.org/10.1016/S0001-706X(98)00078-3).
 48. Arumugam TU, Takeo S, Yamasaki T, Thonkuiatkul A, Miura K, Otsuki H, Zhou H, Long CA, Sattabongkot J, Thompson J, Wilson DW, Beeson JG, Healer J, Crabb BS, Cowman AF, Torii M, Tsuboi T. 2011. Discovery of GAMA, a *Plasmodium falciparum* merozoite micronemal protein, as a novel blood-stage vaccine candidate antigen. Infect Immun 79:4523–4532. <https://doi.org/10.1128/IAI.05412-11>.
 49. Mehrizi AA, Rezvani N, Zakeri S, Gholami A, Babaeekhou L. 2018. Poly(I:C) adjuvant strongly enhances parasite-inhibitory antibodies and Th1 response against *Plasmodium falciparum* merozoite surface protein-1 (42-kDa fragment) in BALB/c mice. Med Microbiol Immunol 207:151–166. <https://doi.org/10.1007/s00430-018-0535-4>.
 50. Chen JH, Jung JW, Wang Y, Ha KS, Lu F, Lim CS, Takeo S, Tsuboi T, Han ET. 2010. Immunoproteomics profiling of blood stage *Plasmodium vivax* infection by high-throughput screening assays. J Proteome Res 9: 6479–6489. <https://doi.org/10.1021/pr100705g>.
 51. Kassegne K, Abe EM, Chen JH, Zhou XN. 2016. Immunomic approaches for antigen discovery of human parasites. Expert Rev Proteomics 13:1091–1101. <https://doi.org/10.1080/14789450.2016.1252675>.